OLIGONUCLEOTIDES 18:245–256 (2008)

DOI: 10.1089/oli.2008.0126

An Efficient Biodelivery System for Antisense Polyamide Nucleic Acid (PNA)

Mohamed Mehiri,[1] Gregory Upert,[1] Snehlata Tripathi,[2] Audrey Di Giorgio,[1] Roger Condom,[1] Virendra N. Pandey,[2] and Nadia Patino[1]

With the aim of developing a general and straightforward procedure for the intracellular delivery of naked peptide nucleic acids (PNAs), we designed an intracellularly biodegradable triphenylphosphonium (TPP) cation based transporter system. In this system, TPP is linked, via a biolabile disulfide bridge, to an activated mercaptoethoxycarbonyl moiety, allowing its direct coupling to the N-terminal extremity of a free PNA through a carbamate bond. We found that such TPP-PNA-carbamate conjugates were highly stable in a cell culture medium containing fetal calf serum. In a glutathione-containing medium mimicking the cytosol, the conjugates were rapidly degraded into an unstable intermediate, which spontaneously decomposed, releasing the free PNA. Using a fluorescence-labeled PNA–TPP conjugate, we demonstrated that conjugates were taken up by cells. Efficient cellular uptake and release of the PNA into the cytosol was further confirmed by the anti-HIV activity measured for the TPP-conjugate of a 16-mer PNA targeting the TAR region of the HIV-1 genome. This conjugate exhibited an IC_{50} value of 1 μM, while the free 16-mer PNA did not inhibit replication of HIV in the same cellular test.

Introduction

Peptide nucleic acids (PNA) are DNA/RNA surrogates that hybridize to complementary DNA and RNA sequences having remarkably high specificity and affinity (Shabih et al., 2006). PNAs are constituted by an achiral, uncharged pseudopeptide backbone that makes them extremely stable in biological fluids. Despite their strong potential as antigene and antisense agents, their clinical use is hampered by their poor intrinsic uptake by cells. Unlike negatively charged oligonucleotide, PNA being uncharged cannot be delivered using cationic lipids (Resina et al., 2007).

Several methods have been devised to enhance the efficiency of PNA delivery, including (1) their covalent conjugation, directly or via a linker, to carriers such as neutral or cationic lipophilic molecules, cell-penetrating peptides, and cell-specific receptor ligands or (2) their adsorption onto polymeric microspheres or (3) their encapsulation in autologous erythrocytes (Koppelhus and Nielsen, 2003; Chiarantini et al., 2005). However, these strategies led to the intracellular release of a modified PNA linked at one extremity to a residual entity that could alter the antigene or antisense properties of the corresponding free PNA. Moreover, the cellular antigene and antisense potency of PNAs is closely linked to the cell import mechanism (passive diffusion, cell-receptor-mediated active transport, or endocytosis) of the PNA-carrier conjugates. This mechanism depends mainly not only on the chemical nature of the carrier, but it also depends on parameters such as the nature of the spacer linking the PNA to the carrier or the localization of the carrier on the PNA (Bendifallah et al., 2003, 2006; Wolf et al., 2006; Abes et al., 2007; Lebleu et al., 2008). Another major drawback associated with PNA-carrier conjugates is the difficulty of their preparation.

There is great need for a general and straightforward procedure that would lead to PNA-carrier conjugates from which efficient delivery of unmodified PNAs can be intracellularly triggered. To circumvent the drawbacks and meet this need, we have designed, on the basis of the works described by Murphy et al. (Muratovska et al., 2001; Filipovska et al., 2004), an easy-to-perform PNA delivery protocol, illustrated in Figure 1, which is based on the attachment of PNA to the lipophilic triphenylphosphonium (TPP) cation through an

[1]Laboratoire de Chimie des Molécules Bioactives et des Arômes (LCMBA), Université de Nice-Sophia Antipolis-CNRS, Institut de Chimie de Nice, Nice, France.
[2]Department of Biochemistry and Molecular Biology, New Jersey Medical School, University of Medicine and Dentistry of New Jersey, Newark, New Jersey.

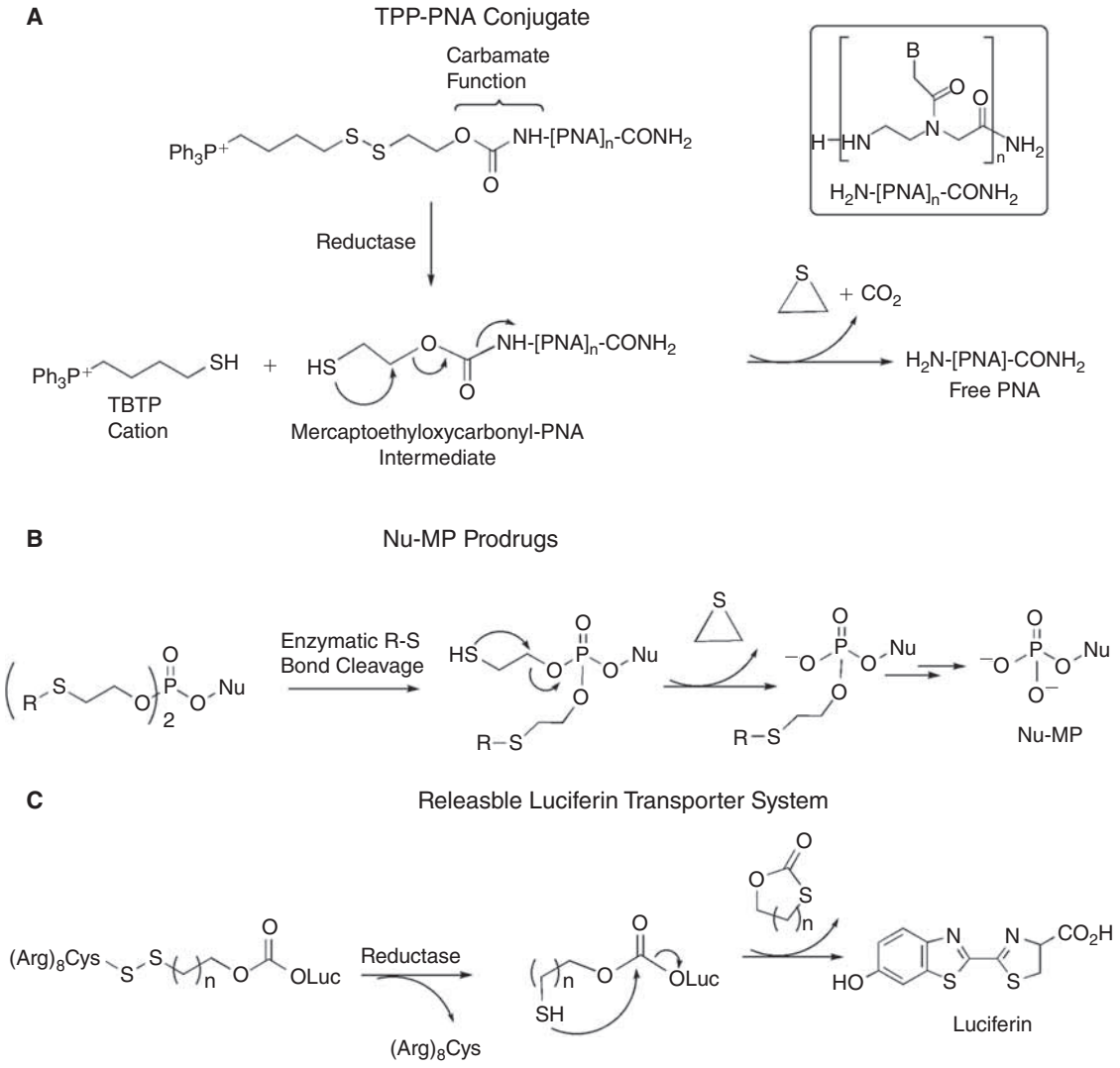

FIG. 1. Strategies for improving the intracellular delivery of cargo molecules or drugs. (**A**) Mechanism of PNA release from PNA–TPP conjugates; (**B**) mechanism of nucleoside monophosphate release from Nu-MP prodrugs; (**C**) mechanism of luciferin release from polyArg-luciferin conjugate.

intracellularly biodegradable carbamate linker containing a disulfide bridge. The TPP moiety was selected for its ability to facilitate the lipid bilayer transport of PNA conjugates, driven by the membrane potential (Muratovska et al., 2001; Filipovska et al., 2004). Once in the cytosol, the intracellular glutathione pool is expected rapidly to reduce the disulfide bond, giving rise to the thiobutyltriphenyl cation (TBTP) and to the unstable mercaptoethyloxycarbamate-PNA intermediate, which further decomposes, thus leading to the release of free PNA (Fig. 1A). As previously demonstrated by Murphy et al. (Filipovska et al., 2004), the cleavage of the disulfide bridge and, consequently, the loss of the TBTP moiety occurring in the reducing environment of cytosol is essential to avoid redistribution of the TPP-PNA conjugate into mitochondria.

This strategy has some similarities to that reported for promoting the intracellular release of anti-HIV active nucleoside monophosphates (Nu-MP) from phosphotriesters incorporating an enzymatically biodegradable protective agent (Fig. 1B; Lefebvre et al., 1995). However, it is more closely related to the recently described releasable transporter system shown in Figure 1C (Jones et al., 2006), which has proven efficiency in the *in vitro* intracellular delivery of luciferin used as cargo model but not in the delivery of PNAs. Luciferin is linked to the biodegradable carrier system through a carbonate bond known to be highly sensitive to hydrolysis. For this reason, the system is quite unstable in biological media, thus limiting its *in vivo* use and its potential as an intracellular delivery system. In our case, the releasable TPP carrier system and the N-extremity of PNA are linked together via a carbamate group that, in contrast to the carbonate one, is known to be more stable in acidic or basic media and less sensitive to enzymatic hydrolysis.

To evaluate the efficiency of our strategy for improving the intracellular delivery of PNAs, we designed and synthesized the ready-to-use activated TPP-based carrier 1 and the

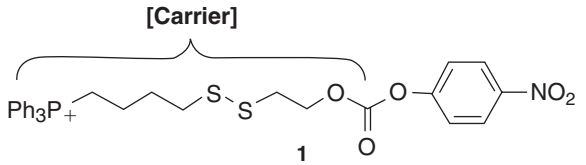

[Carrier]-NH-$[PNA]_{TAR}$-$CONH_2$ **2**

[Carrier]-NH-$[PNA]_{TAR}$-CONHLys(Nε-Fluo)$CONH_2$ **3**

[Carrier]-NH-$[PNA]_2$-$CONH_2$ **4**

$[PNA]_{TAR}$ = 5′-TCCCAGGCTCAGATCT-3′

$[PNA]_2$ = 5′-TC-3′

FIG. 2. Structures of PNA–TPP conjugates synthesized, starting from compound **1**.

PNA conjugate 2, which contained a 16-mer PNA_{TAR} targeting the apical stem-loop TAR RNA of the HIV-1 genome (Fig. 2). This PNA_{TAR} sequence was selected for its ability to inhibit the production of HIV-1 virions in chronically infected cells when conjugated with cell-penetrating peptides (Chaubey et al., 2005; Tripathi et al., 2005). Here we report the synthesis of the TPP-based carrier 1 of the PNA_{TAR}-TPP conjugate 2 and of its fluorescein-labeled analog 3 (Fig. 2), the cellular uptake of 3, and the anti-HIV activity of 2. We report also on the chemical stability and release of free PNA from the diPNA-TPP conjugate 4, taken as a model, when incubated in a cell culture buffer and in a medium mimicking the intracellular compartment.

Materials and Methods

Chemical synthesis

Reagents and solvents were obtained from commercial sources and used without further purification unless indicated. TBTP 5 was synthesized as described elsewhere (Mehiri et al., 2007). 6-O-(carboxymethyl)fluorescein ethyl ester (Flu-OH) and N-α-Boc-Lys(N-ε-Flu)-OH were prepared as described by Lohse et al. (1997). PNA monomers Boc(T)OH, Boc(C^Z)OH, Boc(G^Z)OH, and Boc(A^Z)OH were synthesized as described elsewhere (Meltzer et al. 1995; Coull et al., 1996; Aldrian-Herrada et al., 1998). Analytical thin-layer chromatography was conducted on Merck precoated silica gel 60 F254 plates. The compounds were visualized with Ellman reagent and/or by visualization under ultraviolet light (254 nm and/or 365 nm). Chromatography was performed on Merck silica gel 60 (230–400 mesh ASTM). Analytical and semipreparative HPLC chromatograms were obtained using an HP1100 (UV detector set at 260 nm) and a Beckman (250 × 4 mm) RP-C_{18} (5 μm) column. The HPLC flow rate was 1 mL/min (2 mL/min for semipreparative purification). Elution solvent A was water (0.1% TFA); elution solvent B was acetonitrile (0.1% TFA). ^1H and ^{13}C NMR measurements were done on Brucker AC 200 or AC 500 Fourier transform spectrometers. Chemical shifts (d) are reported in part per million (ppm); for ^1H NMR: s, singlet; d, doublet; t, triplet; q, quartet; m, multiplet; br s, broad resonance. ESI mass spectra were recorded with a Bruker Esquire 3000 plus. MALDI-TOF-MS spectra were recorded with a MALDI-TOF DE PRO Applied Biosystem.

Structures of compounds **1–10** are shown in Figure 3.

Compound 1: Pyridine (53 μL, 0.65 mmol) and 4-nitrophenyl chloroformate (125 mg, 0.62 mmol) were added to a cold (0°C) solution of compound **7** (300 mg, 0.59 mmol) in 5 mL of anhydrous CH_2Cl_2. The mixture was refluxed at 65°C for 5 hours. The solvents were then removed in vacuo and the residue was purified by column chromatography (EtOAc to EtOAc/MeOH 8:2) to yield compound **1** (250 mg, 63%) as a yellowish resin. TLC (EtOAc/MeOH 8:2) Rf 0.42. HPLC (A/B 80:20 to 0:100 over 30 minutes) Rt = 22.0 minutes (λ_{max} = 218 and 267 nm). ^1H NMR (200 MHz, $CDCl_3$, δ) 8.25 (d, 2H, ^3J = 9.2 Hz, H_2, H_6); 8.04-7.57 (m, 15H, PPh_3); 7.38 (d, 2H, ^3J = 9.2 Hz, H_3, H_5); 4.51 (t, 2H, CH_2-O, ^3J = 6.4 Hz); 4.04-3.78 (m, 2H, P-CH_2); 3.08-2.80 (m, 4H, CH_2-CH_2-OH, Ph_3P-$(CH_2)_3$-CH_2-SH); 2.24-2.01 (m, 2H, Ph_3P-$(CH_2)_2$-CH_2); 1.91-1.61 (m, 2H, Ph_3P-CH_2-CH_2). ^{13}C NMR (50.3 MHz, $CDCl_3$, δ) 155.4 (1C (C1)); 152.4 (1C (OCO)); 145.5 (1C (C4); 135.1 (3C (CH_{para})); 133.8 (d, $6CH_{meta}$, J = 9.9 Hz); 130.6 (d, $6CH_{ortho}$, J = 12.4 Hz); 125.4 (2C (C2, C6)); 122.0 (2C (C3, C5)); 118.2 (d, 3C (Ph), J = 86 Hz); 67.0 (CH_2-OH); 37.7 (CH_2-CH_2-OH); 36.5 (Ph_3P-$(CH_2)_3$-CH_2-SH);

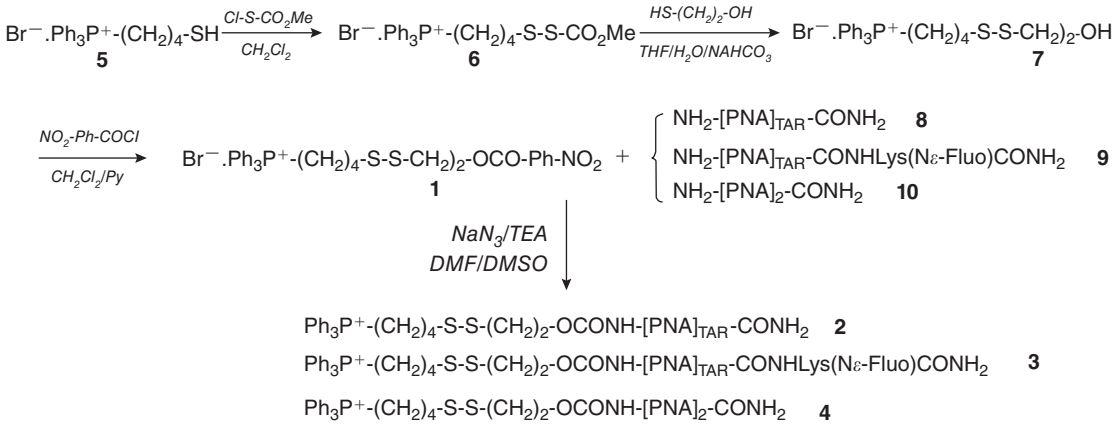

FIG. 3. Synthesis of compounds **1–4**.

29.0 (d, J = 16.8 Hz, Ph_3P-$(CH_2)_2$-CH_2); 22.3 (d, J = 50.5 Hz, Ph_3P-CH_2); 21.0 (d, J = 4.0 Hz, Ph_3P-CH_2-CH_2). ^{31}P NMR (81 MHz, $CDCl_3$, δ) 23.52. MS (ESI+) Calcd for $C_{31}H_{31}NO_5PS_2^+$ $[M]^+$: 592.1. Found: 592.1 $[M]^+$.

[Carrier]-NH-[PNA]-NH_2 2–4. TEA (18 μL, 0.13 mmol) and 300 μL of a NMP solution containing **1** (11.60 mg, 0.017 mmol) and NaN_3 (1.12 mg, 0.017 mmol) were added to a cold solution (0°C) of NH_2-[PNA]-NH_2 **8–10** (0.0086 mmol) in 3 mL of a mixture of NMP/DMSO (9/1, v/v). The mixture was stirred for 30 minutes at this temperature, then allowed to warm to room temperature (ca. 12 hours). Cold diethyl ether (10 mL) was added to the mixture. The crude product was isolated by centrifugation (3000 min^{-1}, –4°C) and washed twice with diethyl ether (10 mL). It was further purified on a reverse-phase HPLC column to give compounds **2–4** after lyophilization.

Compound 2: 18% yield (white solid); HPLC (A/B 100:0 for 5 minutes, then 100:0 to 0:100 over 30 minutes, 1 mL/min, 55°C) Rt = 19.7 minutes. MALDI-TOF-MS Calcd for $C_{195}H_{241}N_{89}O_{51}PS_2^+$ $[M]^+$: 4739.8. Found $[M]^+$: 4740.8.

Compound 3: 6% yield (green fluorescent solid); HPLC (A/B 100:0 for 7 minutes, then 100:0 to 80:20 over 38 minutes, 1 mL/min, 55°C) Rt = 20.6 minutes; MALDI-TOF-MS Calcd for $C_{223}H_{265}N_{91}O_{58}PS_2^+$ $[M]^+$: 5239.9. Found $[M]^+$: 5240.8.

Compound 4: 45% yield (white solid); HPLC (A/B 100:0 to 0:100 over 30 minutes) Rt = 18.4 minutes (λ_{max} = 267 nm); MS (ESI+) Calcd for $C_{46}H_{56}N_{10}O_9PS_2^+$ $[M]^+$: 987.3. Found: 987.3 $[M]^+$.

Compound 6: Methoxycarbonylsulfenyl chloride (231 μL, 2.55 mmol) was added to a cold (0°C) solution of TBTP **5** (1.0 g, 2.32 mmol) in 5 mL of anhydrous CH_2Cl_2. The mixture was stirred for 5 minutes at this temperature, then allowed to warm to room temperature (ca. 4 hours). The residue was taken up in CH_2Cl_2 and washed successively with a 1 M aqueous $KHSO_4$ solution, a saturated aqueous $NaHCO_3$ solution, and a saturated aqueous NaBr solution, then dried over Na_2SO_4. The solvent was removed in vacuo and the residue was purified by column chromatography (EtOAc to EtOAc/MeOH 9:1) to yield compound **6** (850 mg, 65%) as a yellowish resin. TLC (EtOAc/MeOH 8:2) Rf 0.33. HPLC (A/B 80:20 to 0:100 over 30 minutes) Rt = 20.1 minutes (λ_{max} = 224 and 267 nm). ^1H NMR (200 MHz, $CDCl_3$, δ) 7.97-7.54 (m, 15H, PPh_3); 3.94-3.63 (m, 2H, P-CH_2); 3.78 (s, 3H, OMe); 2.81 (t, 2H, CH_2-SH, ^3J = 6.2 Hz); 2.05-1.92 (m, 2H, CH_2-CH_2-SH); 1.90-1.60 (m, 2H, PPh_3-CH_2-CH_2). ^{13}C NMR (50.3 MHz, $CDCl_3$, δ) 170.3 (1C (C=O)); 135.0 (d, $3CH_{para}$, J = 2.9 Hz); 133.7 (d, $6CH_{meta}$, J = 10.2 Hz); 130.5 (d, $6CH_{ortho}$, J = 12.4 Hz); 118.1 (d, 3C (Ph), J = 85.4 Hz); 55.5 (OCH_3); 38.4 (CH_2-SH); 28.2 (d, CH_2-CH_2-SH, J = 17.1 Hz); 22.2 (d, P-CH_2, J = 50.5 Hz); 20.6 (d, P-CH_2-CH_2, J = 4.0 Hz). ^{31}P NMR (81 MHz, $CDCl_3$, δ) 23.57. MS (ESI+) Calcd for $C_{24}H_{26}O_2PS_2^+$ $[M]^+$: 441.1. Found: 441.0 $[M]^+$.

Compound 7: One milliliter of an aqueous solution obtained by mixing 2-mercaptoethanol (59 μL, 0.84 mmol) and $NaHCO_3$ (71 mg, 0.84 mmol) was added to a cold solution (0°C) of compound **6** (420 mg, 0.80 mmol) in 5 mL of THF. The mixture was stirred for 30 minutes at this temperature, then allowed to warm to room temperature (ca. 3 hours). The solvents were removed in vacuo and the residue was purified by column chromatography (EtOAc to EtOAc/MeOH 9:1) to yield compound **7** (350 mg, 86%) as a white resin. TLC (EtOAc/MeOH 8:2) Rf 0.12. HPLC (A/B 80:20 to 0:100 over 30 minutes) Rt = 15.9 minutes (λ_{max} = 240 and 267 nm). ^1H NMR (200 MHz, $CDCl_3$, δ) 8.01-7.54 (m, 15H, PPh_3); 4.13 (bs, 1H, OH); 3.94-3.64 (m, 4H, P-CH_2 and CH_2-OH); 2.86 (t, 2H, ^3J = 6.12 Hz, CH_2-CH_2-OH); 2.81 (t, 2H, ^3J = 6.12 Hz, Ph_3P- $(CH_2)_3$-CH_2-SH); 2.21-1.93 (m, 2H, Ph_3P-$(CH_2)_2$-CH_2-CH_2-SH); 1.89–1.61 (m, 2H, Ph_3P-CH_2-CH_2-CH_2). ^{13}C NMR (50.3 MHz, $CDCl_3$, δ) 135.1 (d, $3CH_{para}$, J = 2.9 Hz); 133.7 (d, $6CH_{meta}$, J = 10.2 Hz); 130.6 (d, $6CH_{ortho}$, J = 12.4 Hz); 118.2 (d, 3C (Ph), J = 85.6 Hz); 59.9 (CH_2-OH); 42.0 (CH_2-CH_2-OH); 37.8 (Ph_3P-$(CH_2)_3$-CH_2-SH); 29.8 (d, J = 16.5 Hz, Ph_3P-$(CH_2)_2$-CH_2-CH_2-SH); 22.3 (d, J = 50.5 Hz, Ph_3P-CH_2); 21.0 (d, J = 4.0 Hz, Ph_3P-CH_2-CH_2). ^{31}P NMR (81 MHz, $CDCl_3$) δ 25.5. MS (ESI+) Calcd for $C_{24}H_{28}BrOPS_2^+$ $[M]^+$: 427.1. Found: 426.9 $[M]^+$.

PNA 8–10: PNA **8–10** were prepared by a solid-phase strategy. They were synthesized in a 20-mL glass peptide vessel fitted with a polyethylene filter disk. Solvents and soluble reagents were removed by filtration under nitrogen. All syntheses and washes were done at 25°C.

PNA oligomers were synthesized on an MBHA resin LL (100–200 mesh, 0.40–0.80 mmol/g, Novabiochem), which was downloaded to approximately half of its maximal capacity for the first building block. The remaining sites were capped using the capping mixture described below. PNA oligomers **8–10** were typically synthesized on 250 mg of resin using a standard Boc/Z protocol:

Boc cleavage: TFA/TIS 90:10, 2*15 minutes, DCM wash, NMP wash.

Coupling: The couplings were done for 1 hours 30 minutes with a volume of 1.5 mL of a preactivated (3 minutes) mixture of PNA monomer (3.6 equiv), DIEA (9 equiv), and HBTU (3.5 equiv) in NMP. For Boc(G^Z)OH, a mixture of NMP/DMSO (4/1, v/v) was used. Couplings were monitored by the Kaiser test and repeated until complete.

Capping: Ac_2O/Pyr/NMP 5:10:85, 5 minutes, DCM wash, NMP wash.

Cleavage of compounds 2–4 from the resin: This was achieved by using a low-high TFMSA protocol using TFMSA/TFA/TIS (1:8:1) for 4 hours. The liquid phase, plus TFA (1 mL) from washing the resin, was added to cold anhydrous diethyl ether (8 mL). Crude PNA oligomer was isolated by centrifugation (3000 min^{-1}, –4°C), washed twice with diethyl ether (8 mL), and used in the next step without further purification.

NH_2-$[PNA]_{TAR}$-$CONH_2$ 8: 134 mg of crude compound **8** with a purity of 30% as determined by HPLC (A/B 100/0 for 7 minutes, then 0/100 to 50/50 over 45 minutes, 55°C) Rt = 20.0 minutes. MALDI-TOF-MS Calcd for $C_{170}H_{215}N_{89}O_{49}$ $[M + H]^+$: 4286.7. Found $[M + H]^+$: 4287.2.

NH_2-$[PNA]_{TAR}$-CONHLys(Nε-Fluo)$CONH_2$ 9: 120 mg of crude **9** with a purity of 95% as determined by HPLC (A/B 100:0 for 7 minutes, then 100:0 to 80:20 over 45 minutes, 1 mL/mn, 55°C) Rt = 13.5 minutes. MALDI-TOF-MS Calcd for $C_{200}H_{243}N_{91}O_{56}$ $[M + H]^+$: 4814.9. Found $[M + H]^+$: 4814.5.

NH_2-[TC]-$CONH_2$ 10: 42 mg of crude compound 10 with a purity of 95% as determined by HPLC (A/B 100/0 to 0/100 over 30 minutes) Rt = 9.4 minutes. MS (ESI+) Calcd for $C_{21}H_{30}N_{10}O_7$ $[M + H]^+$: 535.2. Found: 535.2 $[M + H]^+$.

Stability and decomposition studies

Stability of diPNA–TPP conjugate 4 in a 10% FCS/RPMI medium. Compound **4** (0.8 mg, 0.81 mM) was dissolved in 1 mL of a 10% FCS/RPMI solution (pH 7.4), which was then divided up into 20 microfuge tubes (50 μL each). Incubation was performed at 37°. At appropriate times, 50 μL of methanol was added, and the solution was centrifuged (3000 min^{-1}, –4°C). Subsequently, 20 μL of the supernatant were analyzed by HPLC (A/B 100:0 to 0:100 over 30 minutes).

Cell-free assays for the release of PNA 10 from conjugate 4. Compound **4** (0.8 mg, 0.81 mM) was dissolved in 1 mL of RPMI containing 1 mg of glutathione. The pH was adjusted to 7.4 using 0.1 N NaOH. The solution was divided into twenty 50 μL microfuge tubes at 0°C. Incubation was performed at 37°C. At appropriate times (every 15 minutes during 2.5 hours), 5 μL of TFA was added and 20 μL of the solution was analyzed by HPLC (A/B 100:0 to 0:100 over 30 minutes).

Flow cytometric determination of cellular uptake. CEM cells were incubated with 500 nM of fluo-PNA_{TAR}-TPP conjugate 3 for 6 hours in complete RPMI media with 10% FCS and grown as above. Cells were harvested, washed several times with PBS, and then resuspended in RPMI media containing 2% FCS. Flow cytometry analyses (Beckton Dickinson flow cytometer) were carried out in the presence of 1 μg of propidium iodide/mL to exclude nonviable cells. Cell Quest Pro software (Beckton Dickinson) was used to acquire and analyze the events by the FL1 detector (for fluorescein-labeled conjugate), which excluded FL3 detector (propidium iodide).

Gel retardation assay

Gel retardation assay was done to determine the specificity of PNA_{TAR}-TPP conjugate 2 for HIV-1 TAR sequences. The 5′^{32}P-labeled 82-mer TAR DNA (50 nM) was incubated with increasing concentration of PNA_{TAR}-TPP conjugate 2 in the binding buffer as described before (18). After 30 minutes of incubation at room temperature, equal volume of gel loading dye (0.2% bromophenol blue and 20% glycerol) was added and the samples were subjected to gel electrophoresis on an 8% native polyacrylamide gel as described before (Planelles et al., 1995). The retardation in the mobility of the labeled TAR DNA due to its binding to PNA_{TAR} was detected by PhosphorImager analysis of the gel (Molecular Dynamics, Sunnyvale, CA, USA).

Antiviral activity of PNA_{TAR}-TPP conjugate 2

The CEM cells grown in mid-log phase were infected with pseudotyped HIV-1 virions competent for one-cycle infection. The pseudotyped HIV-1 virions harboring luciferase reporter gene were produced in 293T cells by cotransfecting them with pHIV-$1_{JR\text{-}CSF\text{-}luc}$env(–) and pVSV-G as described earlier (Planelles et al., 1995). The infection was performed by incubating 1×10^6 cells with pseudotyped HIV-1 virions (equivalent to 14 ng of p24) at 37°C for 2 hours. The infected cells were centrifuged, washed with PBS without Ca^{2+} or Mg^{2+}, and resuspended in complete RPMI medium in a 12-well plate. The infected cells were then grown in the presence of increasing concentrations of PNA_{TAR}-TPP conjugate **2** in the complete medium supplemented with 1% DMSO. PNA_{TAR}-alone, TBTP **5,** and TBTP-mercaptoethanol **7** (TBTP-M) cations (without PNA) were used as negative controls. After 48 hours of incubation, cells were harvested, washed, and lysed in passive lysis buffer (Promega, Madison, WI, USA) by gentle rocking for 15 minutes. An aliquot of the lysate was used for determining the expression of luciferase activity using the Luciferase Assay Reagent from Promega as previously described **(**Tripathi et al., 2005, 2007). The percent inhibition of expression of luciferase activity in the presence and absence of PNA_{TAR}-TPP conjugate **2** was determined. The median-dose effect (IC_{50}) was calculated using CalcuSyn software (BIOSOFT, Cambridge, UK). This software, developed by Chou (Chou, 1974, 1977), is used for dose-effect analysis and determination of IC_{50} of drugs.

Evaluation of cytotoxicity of delivery vector (TBTP 5) and its derivative (TBTP-M 7) by [^{3}H] thymidine incorporation assay

The CEM cells in 24 well plates (1×10^5 cells/well) were grown in the absence and presence of 1% DMSO in complete RPMI medium containing 1 and 2 μM of TBTP 5 vector and its derivative, TBTP-M 7. The culture media was supplemented with 2.5 μCi of [methyl-3H] thymidine. Cells were harvested at different time points, washed with PBS, and resuspended in 200 μL of lysis buffer (1% NP-40 in PBS). The genetic material was precipitated by 10% tricholoroacetic acid (TCA), collected on glass fiber filter, washed with the TCA and 70% ethanol. The filters were dried in air and counted for radioactivity in a liquid scintillation counter. The total protein in each lysate was determined by using Bio-Rad assay, and incorporation of ^{3}H-thymidine was calculated as counts per minute (cpm) per mg of protein.

Results

Chemistry

Synthesis of the PNA conjugates **2–4,** described in Figure 3, first necessitated preparation of the key para-nitrophenyl carbonate synthon **1**. This synthon was obtained in three steps, starting from 4-thiobutyltriphenylphosphonium bromide **5** (TBTP.Br^-) (Mehiri et al., 2007). The thiol group in **5** was activated with methoxycarbonylsulfenyl chloride to give intermediate **6**, which was then reacted with mercaptoethanol to give disulfide derivative **7** (86% yield for these two steps). Condensation of **7** with para-nitrophenylchloroformate gave the ready-to-use compound **1**, in 63% yield after purification by silica gel chromatography. Structures of compound 1 and intermediates 6 and 7 were confirmed by ^{1}H, ^{13}C, ^{31}P NMR, and ESI-MS experiments.

The carbamate PNA-vector conjugates **2–4** were obtained by condensing an excess of the para-nitrophenyl activated carbonate **1** with crude PNA **8–10**. Coupling of the longer PNAs, **8** and **9**, with **1** was effective only upon activation of **1** as its azide form, which was generated *in situ* after the addition of sodium azide. Conjugates **2–4** were easily purified by

semipreparative HPLC, and their structures were confirmed by MALDI-TOF-MS. The PNA sequences **8–10** were synthesized on solid support (MBHA resin) by well-established protocols (see Materials and Methods). For the preparation of conjugate **3**, a N-Boc N-ε fluorescein-labeled lysine residue was introduced on the resin before PNA elongation (Lohse et al., 1997).

Stability of the diPNA-carrier conjugate 4 and release of free diPNA

The chemical stability of the diPNA conjugate **4,** taken as a model of PNA–TPP conjugates, was assessed in an RPMI buffer supplemented with 10% fetal calf serum (pH 7.4) at 37°C, using analytical HPLC. After 48 hours of incubation, no degradation was detected, demonstrating that both the carbamate linker and the disulfide bridge were highly stable in the cell culture medium, very similar to the one used for the inhibition assays. To determine whether the cytoplasmic reduction of the disulfide bond in PNA conjugates **2** and **3** could induce release of the corresponding free PNA, conjugate **4** was incubated at 37°C in an RPMI solution containing glutathione (1 mg/mL; ~3 mM), which mimics the intracellular medium. HPLC analyses showed rapid consumption of **4** into intermediates **11** and **12**, from which free diPNA **10** was released more slowly (Fig. 4). After nearly 1 hours of incubation, only the naked diPNA **10** was detected by HPLC, both with TBTP derivatives **5** and 5-bis (TBTP dimer). Although the intermediate **11** could not be identified by HPLC/MS analyses, it is probably the mercaptoethoxycarbamate-PNA shown in Figure 1, since compound **12** was identified as being the disulfide conjugate of glutathione and mercaptoethoxycarbamate-PNA.

Cellular uptake studies

Cellular uptake of the fluorescein-labeled PNA_{TAR}-TPP conjugate **3** was examined in CEM cells by flow cytometry (FACS analysis) (Fig. 5, panel B and C) in the presence of 1% DMSO in the culture medium. DMSO has been shown to be least toxic of most of the organic chemicals, and at 1% concentration it has no toxicity on the CEM and 293T cells used in the present work. Most of the anti HIV-1 nonnucleoside drugs are tested in cell culture in the presence of 1% DMSO at which viral infectivity and cell viability remained unaffected (Borkow et al., 1997). Briefly, CEM cells were grown as above and incubated with fluo-PNA_{TAR}-TPP conjugate **3** for 6 hours. Cells were harvested, washed, and subjected to FACscan analysis in presence of propidium iodide to exclude dead cells. Approximately 43% cells were found to be fluorescence positive (Fig. 5, panel D). Under similar conditions the cellular uptake of fluorescence labeled naked PNA was shown to be negligible (Chaubey et al., 2007).

*Binding specificity of the PNA_{TAR}-TPP conjugate **2** to TAR DNA*

In order to evaluate the binding affinity of the PNA_{TAR}-TPP conjugate **2** to their target sequence, we performed a gel mobility shift assay with 5′ ^{32}P-labeled 82-base long TAR DNA (50 nM) and increasing concentrations of PNA_{TAR}-TPP conjugate **2** (Fig. 6). It was observed that at 1:2 ratio of PNA_{TAR}-TPP conjugate to TAR DNA, the mobility shift of approximately 50% of the TAR DNA was noted (lane 3) while at an equimolar ratio 100% shift was achieved (lane 4), suggesting stoichiometric interaction of the conjugate with its target sequence.

In vitro *inhibition of HIV-1 replication in the presence of PNA_{TAR}-TPP conjugate **2***

The antiviral activity of PNA_{TAR}-TPP conjugate **2** was investigated in CEM cells. These cells were first infected with pseudotyped HIV-1 virions harboring the luciferase reporter gene, then grown for 48 hours in the presence of increasing concentrations of conjugate **2**. Naked PNA_{TAR}, TBTP, and TBTP-M cations **5** and **7** were used as controls. After incubation, cells were lysed and an aliquot of the cell lysate was examined for luciferase activity as previously described (Tripathi et al., 2005). Luciferase expression in untreated cells was taken as a control and assigned an arbitrary value of 100. The percent inhibition of luciferase expression was determined for the treated samples relative to the untreated control cells. The median-effect dose (IC_{50}) of PNA_{TAR}-TPP conjugate **2** was 1.0 μM (Fig. 7), while both TBTP and TBTP-M had no inhibitory effect on luciferase expression. The linear correlation coefficient (*r*) was 0.97 and r value was found to be 1. PNA_{TAR}-alone had no inhibitory effect; therefore no values can be generated for the dose-effect curve in CalcuSyn software. The luciferase expression was found to be uninhibited in presence of vector TBTP 5 and TBTP-M 7 as well as in presence of PNATAR-alone. PNATAR-alone showed no inhibitory effect on luciferase expression; therefore no value could be put in the dose-effect curve plot of CalcuSyn software.

Toxicity of vector (TBTP) 5 and its derivative (TBTP-M) 7

We examined the cytotoxicity of the cationic delivery vectors in the presence of 1% DMSO by monitoring ^{3}H-thymidine incorporation in the cellular DNA. Cells were grown in the presence of the vector in a medium containing ^{3}H-thymidine and the extent of thymidine incorporation was determined. Results shown in Figure 8 suggest that TBTP and its derivative TBTP-M are welltolerated and therefore nontoxic to the cells at 1–2 μM concentration.

Discussion

With the aim of developing a general and straightforward strategy for the delivery of unmodified PNA into cells, we have developed a convenient three-step procedure for preparation of the TBTP-based compound **1,** in which the TBTP moiety is linked via a disulfide bridge to an activated mercaptoethoxycarbonyl function, allowing its coupling to the amino extremity of the PNA backbone. Compound **1,** which can be stored for several weeks at –4°C without degradation, is, therefore, a powerful and valuable starting material for conjugation to any cargo molecule that has an appropriate

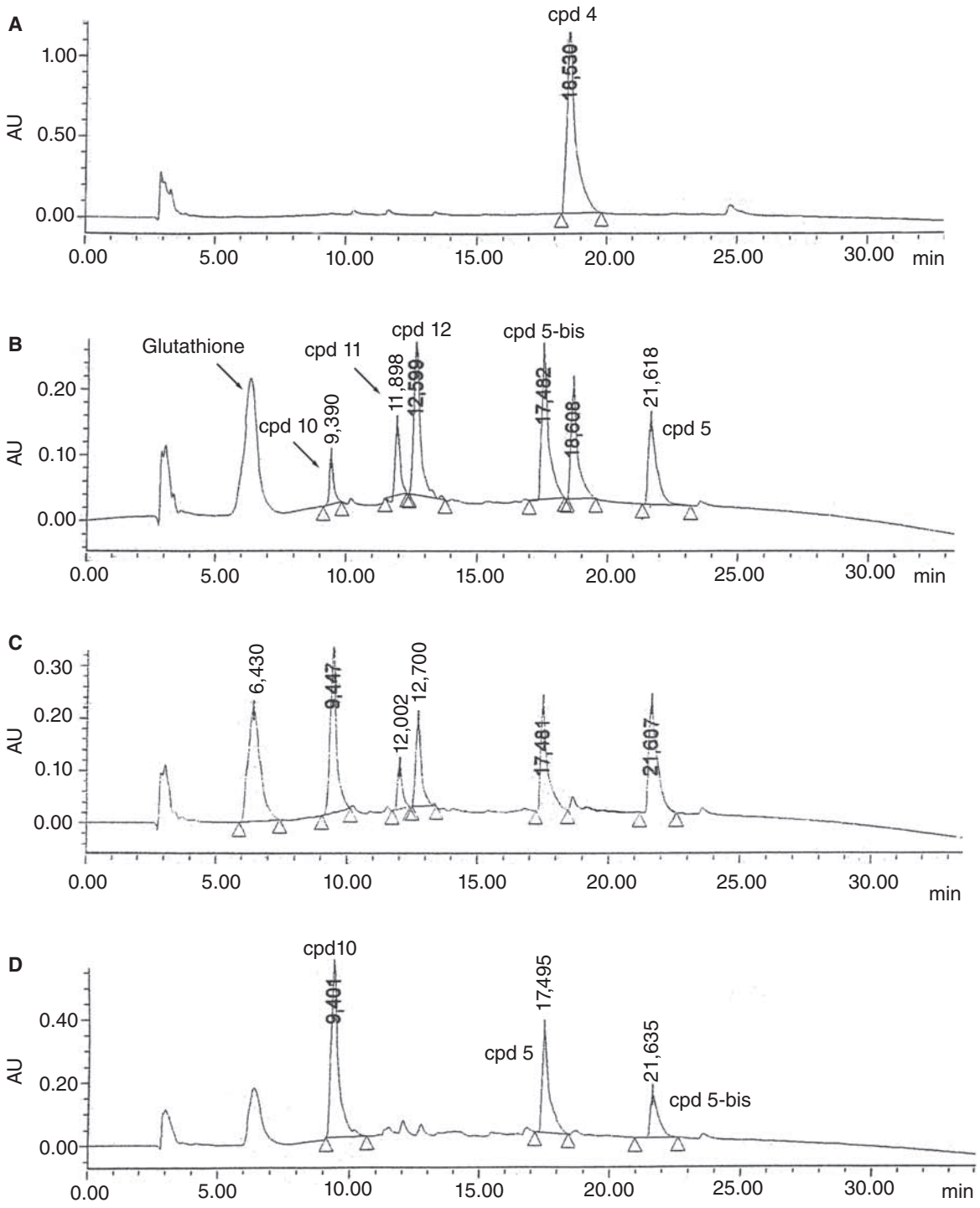

FIG. 4. HPLC traces of (**A**) Compound 4 in a RPMI medium; (**B**) degradation profile of compound 4 after 5 minutes of incubation at 37°C in RPMI containing glutathione medium (3 mM); (**C**) after 15 minutes; (**D**) after 60 minutes. The values shown over each peak are times of elution. [HPLC conditions: Beckman (250Z4 mm) RP-C18 (5 μm) column; solvent A :(1% TFA) H_2O, solvent B: (1% TFA) CH3CN; A/B from 0/100 to 100/0 in 35 minutes; flow rate: 1 mL/min; 214 nm].

chemical function, is of biological interest, and has poor cell permeation properties.

In the present study, we obtained PNA–TPP conjugates in one step, starting from compound **1** and unpurified crude PNA preparations. Indeed, as shown for PNATAR **8** (Fig. 9A), the crude HPLC chromatogram reveals multiple impurities, some of them masked under the signal corresponding to the expected product. The HPLC purification of

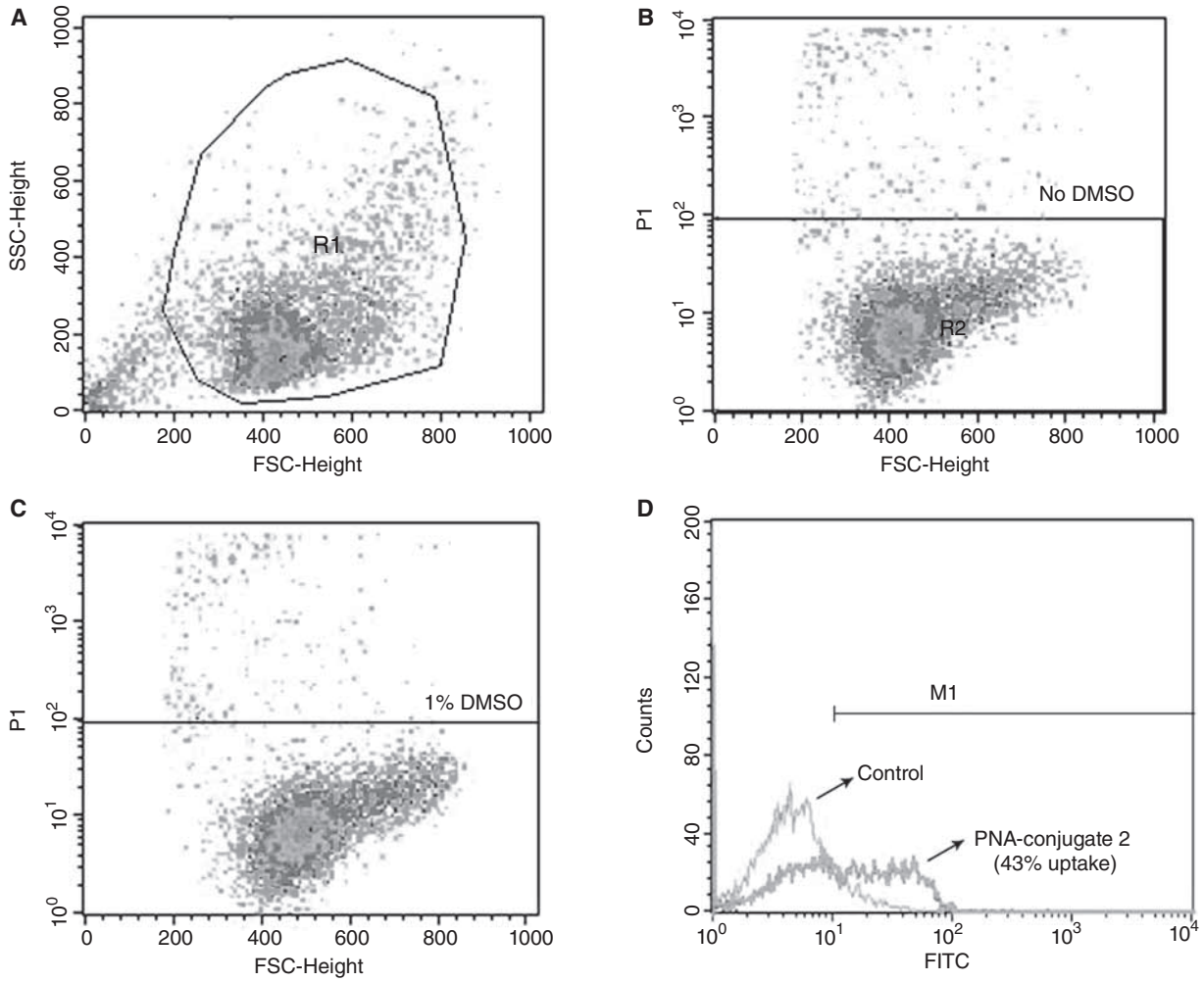

FIG. 5. Cellular uptake of the fluo-PNATAR-TPP conjugate **3** by flow cytometry analysis: CEM cells were incubated with the fluorescein-labeled conjugate for 6 hours at 37°C. After washing thoroughly with phosphate-buffered saline solution, the cells were resuspended in RPMI media containing 2% FCS. Analysis was done in presence of propidium iodide. Panel A represents cells grown in the absence of DMSO. R1 represents the field of viable cells; panels B and C represent cell grown in the absence of DMSO and in the presence of 1% DMSO, respectively, excluding approximately 4% propidium iodide positive dead cells; panel D shows flow cytometry data of the uptake of conjugate 3 after 6 hours of incubation in presence of 1% DMSO (blue peak), showing 43% uptake as compared to control (green peak).

crude PNAs would therefore be tedious and time consuming, and would lead to loss of the desired product. These impurities likely are N-terminal acetylated deleted PNA sequences, formed during the capping step with the acetic anhydride/pyridine mixture. Consequently, on addition of an excess of compound **1** on a crude PNA-containing solution, all the amino-free PNA present in the mixture are converted into their TPP-conjugate, whereas impurities do not react. Interestingly, the HPLC retention of TPP-conjugates markedly differs from the unconjugated N-terminal acetylated PNA sequences (Fig. 9B), allowing easy and rapid purification of the target compound. Thus, this synthetic strategy is timesaving and leads to an increase in yield.

The stability of such conjugates, and their degradation pathway, were assessed in cell culture medium and in a medium mimicking the intracellular one, with the diPNA–TPP conjugate **4** taken as a model (Fig. 4). When incubated in a 10% FCS/RPMI medium at 37°C, no decomposition occurred, even after 48 hours, demonstrating that both the carbamate linker and the disulfide bond are highly stable under these conditions. Adding glutathione to this medium resulted in cleavage of the disulfide bridge, which induced, as expected, release of the naked diPNA **10** in less than 2 hours. Although no formal demonstration has been provided for the decomposition of PNA–TPP conjugates within cells, our experiments suggest that they should be stable in an extracellular medium, and that they should rapidly decompose into the cells to release free PNA, thus allowing its interaction with its RNA or DNA target located in the cytoplasm or nucleus.

FACscan studies (Fig. 5) demonstrated efficient and rapid internalization of such PNA conjugates into cells. Their

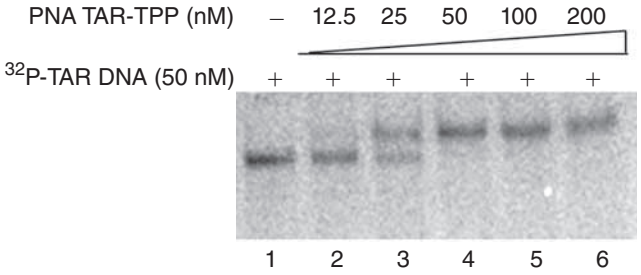

FIG. 6. Specificity of interaction of PNATAR-TPP conjugate **2** with its target sequence on HIV-1 TAR. The ^{32}P-labeled TAR DNA (50 nM) was incubated with the PNATAR-TPP conjugate at different molar ratio of the conjugate followed by gel electrophoresis as described in the Materials and Methods. Lanes 1 is the control without conjugate. Lanes 2 through 6 represent 0. 25, 0.5, 1.0, 2.0, and 4.0 molar ratio of conjugate to TAR DNA.

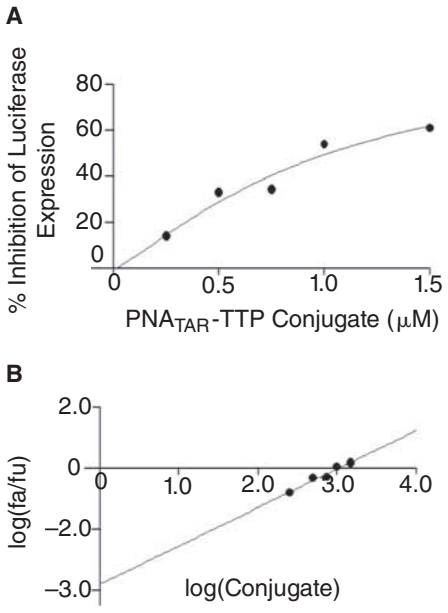

FIG. 7. (**A**) Dose-effect curve for antiviral activity of PNATAR-TPP conjugate **2**. CEM cells were infected with VSV-G pseudotyped S1 strain of HIV-1 and grown in the presence of increasing concentrations of conjugate **2** (0–1500 nM). PNATAR alone, TBTP **5** and TBTP-M **7** were included in the experiment as controls. Cells were harvested, lysed, and assayed for luciferase expression 48 hours after infection. The effect of conjugate **2** concentrations on the luciferase expression was analyzed using CalcuSyn software (Biosoft). (**B**) Median-effect plot: The IC_{50} value, determined from the ratio of log of luciferase expression in treated cells (fa) and untreated cells (fu) as a function of the log concentration of conjugate **2** was $1.0 > M$; the linear correlation coefficient, *r*, was 0.97.

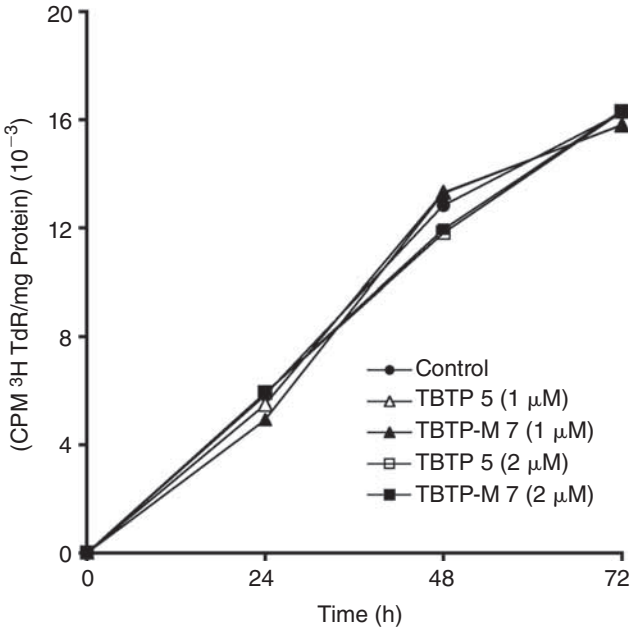

FIG. 8. Effect of vector (TBTP **5**) and its derivative (TBTP-M **7**) on [3H] thymidine incorporation into cellular DNA in CEM cells. Cells were grown in presence of 1% DMSO indicated concentration of vector and its derivative as described in the Materials and Methods. The culture media was supplemented with 2.5 μCi of [methyl-3H] thymidine. The cells were harvested at indicated time points and assayed for [3H]-thymidine (TdR) incorporation in the cellular DNA.

efficient intracellular uptake was further corroborated by the anti-HIV activity found for the PNA$_{TAR}$-TPP conjugate **2**, which carries a 16-mer PNA$_{TAR}$ fragment directed against the TAR RNA region of the HIV genome. Indeed, the TPP-PNA$_{TAR}$-conjugate **2** inhibited HIV replication in CEM cell lines with an IC_{50} value of ~1 micromolar, while the 16-mer PNA$_{TAR}$ alone was inactive in these cellular tests. It should be emphasized that the IC_{50} value for PNA–TPP is close to that obtained with PNA$_{TAR}$-CPP conjugates (IC_{50} from 0.4 to 0.8 μM) (Tripathi et al., 2005), suggesting the potential of this new class of conjugate, which is less expensive and can be readily prepared as compared to PNA–CPP conjugates. Moreover, this observed antiviral activity demonstrates that the PNA$_{TAR}$ is not sequestered in mitochondria, confirming that the disulfide bond has been definitively reduced into the cytoplasm.

In conclusion, we have developed an efficient and useful strategy for facilitating the intracellular delivery of unmodified PNA. This method is based on the key compound **1**, which is easily synthesized from commercial material. This synthon, which can be stored without degradation, can be conjugated to any PNA for which one would like to assess the antisense or antigene potential. This easy-to-perform method is an important improvement over other described protocols, which may facilitate *in vitro* applications of PNAs.

We envisage applying this approach to the delivery and intracellular release of cargo molecules that are of biological interest but have poor cell permeation properties.

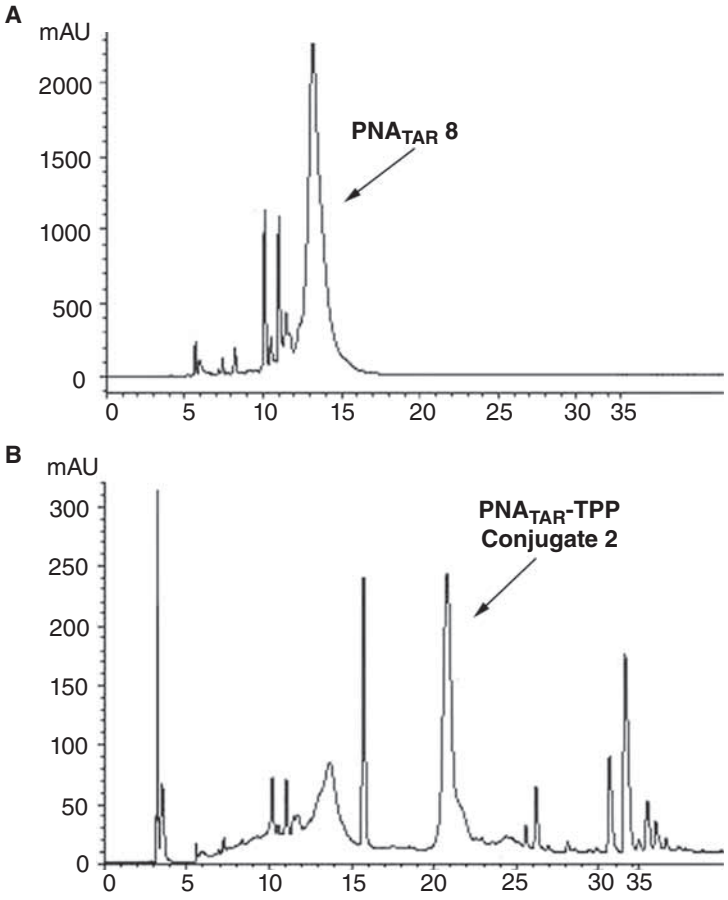

FIG. 9. HPLC traces of PNATAR-TPP conjugate **2** synthesized in one step from crude PNATAR **8** and compound **1**. The unpurified crude PNATAR **8** was incubated with excess of compound **1** at 0°C for 30 minutes with stirring as described in the Materials and Methods. The PNA–TPP conjugate formed in the reaction mixture were precipitated by the addition of cold diethyl ether and purified by HPLC. Panels A and B show HPLC traces of unpurified crude PNATAR as the starting material and PNATAR-TPP conjugate **2** as the reaction product, respectively.

Acknowledgments

This research was supported by grants from Agence Nationale de Recherches sur le SIDA (ANRS) (to R.C.), FIGHT AIDS MONACO (FAM), and the Conseil Général des Alpes–Maritimes (to N.P.), and by a grant from NIH/NIAID (AI 42520) to V.N.P. We also sincerely thank Dr. Beverly E. Barton, Department of Surgery, UMDNJ for carrying out FACScan analysis.

References

ABES, R., ARZUMANOV, A.A., MOULTON, H.M., ABES, S., IVANOVA, G.D., IVERSEN, P.L., GAIT, M.J., and LEBLEU, B. (2007). Cell-penetrating-peptide-based delivery of oligonucleotides: an overview. Biochem. Soc. Trans. **4,** 775–779.

ALDRIAN-HERRADA, G., RABIE, A., WINTERSTEIGER, R., and BRUGIDOU, J. (1998). Solid-phase synthesis of peptide nucleic acid (PNA) monomers and their oligomerization using disulphide anchoring linkers. J. Peptide Sci. **4,** 266–281.

BENDIFALLAH, N., KRISTENSEN, E., DAHL, O., KOPPELHUS, U., and NIELSEN, P.E. (2003) Synthesis and properties of ester-linked peptide nucleic acids prodrug conjugates. Bioconjugate Chem. **14,** 588–592.

BENDIFALLAH, N., RASMUSSEN, F.W., ZACHAR, W., EBBESEN, P., NIELSEN, P.E., and KOPPELHUS, U. (2006). Evaluation of cell-penetrating peptides (CPPs) as vehicles for intracellular delivery of antisense peptide nucleic acid (PNA). Bioconjugate Chem. **17,** 750–758.

BORKOW, G., BARNARD, J., NGUYEN, T.M., BELMONTE, A., WAINBERG, M.A., and PARNIAK, M.A. (1997). Chemical barriers to human immunodeficiency virus type 1 (HIV-1) infection: retrovirucidal activity of UC781, a thiocarboxanilide nonnucleoside inhibitor of HIV-1 reverse transcriptase. J. Virol. **71,** 3023–3030.

CHAUBEY, B., TRIPATHI, S., DESIRE, J., BAUSSANE, I., DECOUT, J.L., and PANDEY, V.N. (2007). Mechanism of RNA cleavage by sequence specific polyamide nucleic acid-neamine conjugate. Oligonucleotides **17,** 302–313.

CHAUBEY, B., TRIPATHI, S., GANGULY, S., HARRIS, D., CASALE, R.A., and PANDEY, V.N. (2005). A PNA-transportan conjugate targeted to the TAR region of the HIV-1 genome exhibits both antiviral and virucidal properties. Virology **331,** 418–428.

CHIARANTINI, L., CERASI, A., FRATERNALE, A., MILLO, E., BENATTI, U., SPARNACCI, K., LAUS, M., BALLESTRI, M., and TONDELLI, L. (2005). Comparison of novel delivery systems for antisense peptide nucleic acids. J. Control Release **109,** 24–36.

CHOU, T.-C. (1974). Relationships between inhibition constants and fractional inhibitions in enzyme-catalysed reactions with different numbers of reactants, different reaction mechanisms, and different types of mechanisms of inhibition. Mol. Pharm. 39, 235–247.

CHOU, T. -C. (1977). Derivation and properties of Michaelis-Menten type and hill equations for reference ligands. J. Theoret. Biol. 272, 16010–16017.

COULL, J.M., EGHOLM, M., HODGE, R.P., ISMAIL, M., and RAJUR, S.B. (1996). Improved synthons for the synthesis and deprotection of peptide nucleic acids under mild conditions. PCT Int. Appl. WO 96/40685.

FILIPOVSKA, A., ECCLES, M.R., SMITH, R.A., and MURPHY, M.P. (2004) Delivery of antisense peptide nucleic acids (PNAs) to the

cytosol by disulphide conjugation to a lipophilic cation. FEBS Lett. **556,** 180–186.

JONES, L.R., GOUN, E.A., SHINDE, R., ROTHBARD, J.B., CONTAG, C.H., and WENDER, P.A. (2006). Releasable luciferin-transporter conjugates: tools for the real-time analysis of cellular uptake and release. J. Am. Chem. Soc. **128,** 6526–6527.

KOPPELHUS, U., and NIELSEN, P.E. (2003). Cellular delivery of peptide nucleic acid (PNA). Adv. Drug Deliver. Rev. **55,** 267–280.

LEBLEU, B., MOULTON, H.M., IVANOVA, G.D., ABES, R., STEIN, D.A., IVERSEN, P.L., ARZUMANOV, A.A., and GAIT, M.J. (2008). Cell penetrating peptide conjugates of steric block oligonucleotides. Adv. Drug Deliv. Rev. **60,** 517–529.

LEFEBVRE, I., PÉRIGAUD, C., POMPON, A., AUBERTIN, A.-M., GIRARDET, J.-L., KIM, A., GOSSELIN, G., and IMBACH, J.-L. (1995). Mononucleoside phosphotriester derivatives with S-acyl-2-thioethyl bioreversible phosphate-protecting groups: intracellular delivery of 3′-azido-2′, 3′-dideoxythymidine 5′-monophosphate. J. Med. Chem. **38,** 3941–3950.

LOHSE, J., NIELSEN, P.E., HARRIT, N., and DAHL, O. (1997). Fluorescein-conjugated lysine monomers for solid phase synthesis of fluorescent peptides and PNA oligomers. Bioconjugate Chem. **8,** 503–509.

MEHIRI, M., CALDARELLI, S., DI GIORGIO, A., BAROUILLET, T., DOGLIO, A., CONDOM, R., and PATINO, N. (2007). A "Ready-To-Use" fluorescent-labelled-cysteine-TBTP (4-thiobutyltriphenylphosphonium) synthon to investigate the delivery of non-permeable PNA (Peptide Nucleic Acids)-based compounds to cells. Bioorganic Chem. **35,** 313–326.

MELTZER, P.C., LIANG, A.Y., and MATSUDAIRA, P. (1995). Peptide nucleic acids: synthesis of thymine, adenine, guanine, and cytosine nucleobases. J. Org. Chem. **60,** 4305–4308.

MURATOVSKA, A., LIGHTOWLERS, R.N., TAYLOR, R.W., TURNBULL, D.M., SMITH, R.A.J., WILCE, J.A., MARTIN, S.W., and MURPHY, M.P. (2001). Targeting peptide nucleic acid (PNA) oligomers to mitochondria within cells by conjugation to lipophilic cations: implications for mitochondrial DNA replication, expression and disease. Nucleic Acids Res. **29,** 1852–1863.

PLANELLES, V., BACHELERIE, F., JOWETT, J.B., HAISLIP, A., XIE, Y., BANOONI, P., MASUDA, T., and CHEN, I.S. (1995). Fate of the human immunodeficiency virus type 1 provirus in infected cells: a role for vpr. J. Virol. **69,** 5883–5889.

RESINA, S., ABES, S., TURNER, J.J., PREVOT, P., TRAVO, A., CLAIR, P., GAIT, M.J., THIERRY, A.R., and LEBLEU, B. (2007). Lipoplex and peptide-based strategies for the delivery of steric-block oligonucleotides. International J. Pharmaceutics **344,** 96–102.

SHABIH, S., SAJJAD, K., and ARIF, A. (2006). Peptide nucleic acid (PNA)—a review. J. Chem. Technol. Biotechnol. **8,** 892–899.

TRIPATHI, S., CHAUBEY, B., GANGULY, S., HARRIS, D., CASALE, R.A., and PANDEY, V.N. (2005). Anti-HIV-1 activity of anti-TAR polyamide nucleic acid conjugated with various membrane transducing peptides. Nucleic Acids Res. 33, 4345–4356.

TRIPATHI, S., CHAUBEY, B., BARTON, B.E., and PANDEY, V.N. (2007). Anti HIV-1 virucidal activity of polyamide nucleic acid-membrane transducing peptide conjugates targeted to primer binding site of HIV-1 genome. Virology 20, 91–103.

WOLF, Y., PRITZ, S., ABES, S., BIENERT, M., LEBLEU, B., and OEHLKE, J. (2006). Structural requirements for cellular uptake and antisense activity of peptide nucleic acids conjugated with various peptides. Biochemistry 45, 14944–14954.

Address correspondence to:
Dr. Virendra N. Pandey
Department of Biochemistry and Molecular Biology
New Jersey Medical School
University of Medicine and Dentistry of New Jersey,
185 South Orange Avenue, Newark, NJ 07103, USA

E-mail: Pandey@umdnj.edu

and

Dr. Nadia Patino
Laboratoire de Chimie des Molécules Bioactives et des Arômes (LCMBA)
UMR 6001 Université de Nice-Sophia Antipolis-CNRS
Institut de Chimie de Nice
28 avenue de Valrose, F06100 Nice, France

E-mail: patino@unice.fr

Received for publication February 9, 2008; accepted after revision March 31, 2008.